Microchip Lasers

J.J. Zayhowski

■ Lincoln Laboratory has developed tunable, single-frequency microchip lasers fabricated from Nd-doped solid state crystals. Diode-laser-pumped Nd:YAG microchip lasers have linewidths of less than 7 kHz at center frequencies of 1.064 and 1.319 μm, and have operated in a single-frequency, single-polarization, fundamental transverse mode at output powers in excess of 50 mW. These lasers have been piezoelectrically tuned over a range of ±300 MHz, with a flat-band tuning response of 0.6 MHz/V at drive frequencies up to 300 kHz. Nd:YAG microchip lasers have also been Q-switched to produce output pulses as short as 6 nsec; much shorter pulses are possible.

Microchip lasers are among the world's smallest and least expensive solid state lasers. At the same time, they have extremely desirable operating characteristics that are difficult to obtain with more conventional designs. For example, microchip lasers are linearly polarized, single-frequency devices that operate in the fundamental transverse mode [1, 2] and can be tuned continuously over the gain bandwidth of the lasing transition [2–4]. The combination of high performance and low cost makes microchip lasers attractive for a wide variety of applications, including fiber-optic communications, optical storage, and medicine.

Basic Microchip Concepts

Microchip lasers are typically fabricated by polishing a wafer of solid state gain medium so that two sides of the wafer are flat and parallel (Figure 1). The thickness of the wafer corresponds to the length of the laser cavity. The polished surfaces are dielectrically coated to form the mirrors of a two-mirror standing-wave laser cavity. The wafer is then diced into small pieces, typically 1 mm square; each piece is a complete microchip laser. As a result of this simple fabrication process and the small amount of material used in each device, microchip lasers have the potential for low-cost mass production. (For an alternative to flat-flat microchip cavities, see the box "Technique for Mass-Producing Microchip Lasers with Curved Mirrors.")

Single-frequency operation of microchip lasers is achieved by making the laser cavity sufficiently short so that the cavity-mode spacing (which is inversely proportional to the cavity length) is comparable to the gain bandwidth of the lasing transition. The cavity length is also chosen so that one of the cavity modes is positioned at the center of the gain and is, therefore, the only mode to see enough gain to reach lasing threshold. Figure 2 illustrates the concept. (For a more detailed discussion, see the box "Single-Frequency Operation of Microchip Lasers" on p. 431.)

In a longitudinally pumped microchip laser, the planar uniformity of the flat-flat cavity is broken by the pump beam, which deposits heat as it pumps the crystal. As the heat diffuses outward from the pump, it forms a thermal waveguide that defines the transverse dimensions of the oscillating mode. These dimensions are larger than the dimensions of the pump field of an unfocused, butt-coupled diode-laser pump. As a result,

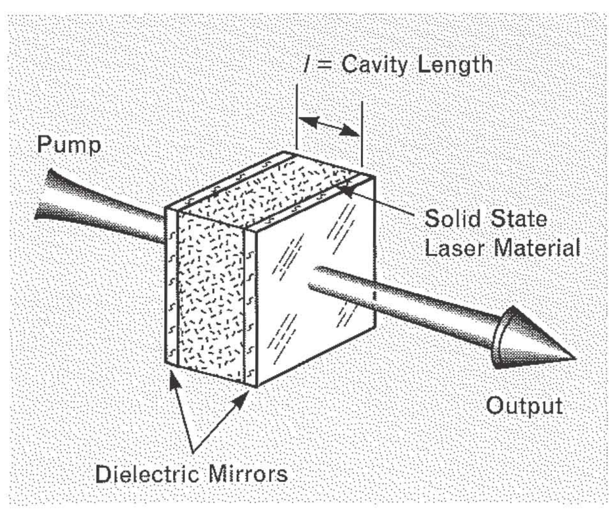

FIGURE 1. Illustration of a microchip laser.

TECHNIQUE FOR MASS-PRODUCING MICROCHIP LASERS WITH CURVED MIRRORS

ONE OF THE attractive aspects of microchip lasers is that they can be fabricated as a cavity bounded by two flat, parallel mirrors. The flat-flat cavity allows for easy manufacturing: large wafers of gain media can be polished and dielectrically coated before they are diced into small sections; each section is a complete laser. The use of a flat-flat cavity, however, does have disadvantages. The gain medium in such a cavity must have a positive change of refractive index with increasing temperature. In addition, the tolerance to misalignment of the two flat mirrors that form the laser cavity is extremely small. For example, the mirror-misalignment tolerance for a Nd:YAG microchip laser is typically 10 μrad. The use of a microchip cavity with at least one curved mirror can increase the tolerance to mirror misalignment and remove the restrictions on the gain medium. Curved mirrors should also reduce the amount of pump power required for the microchip laser to reach threshold.

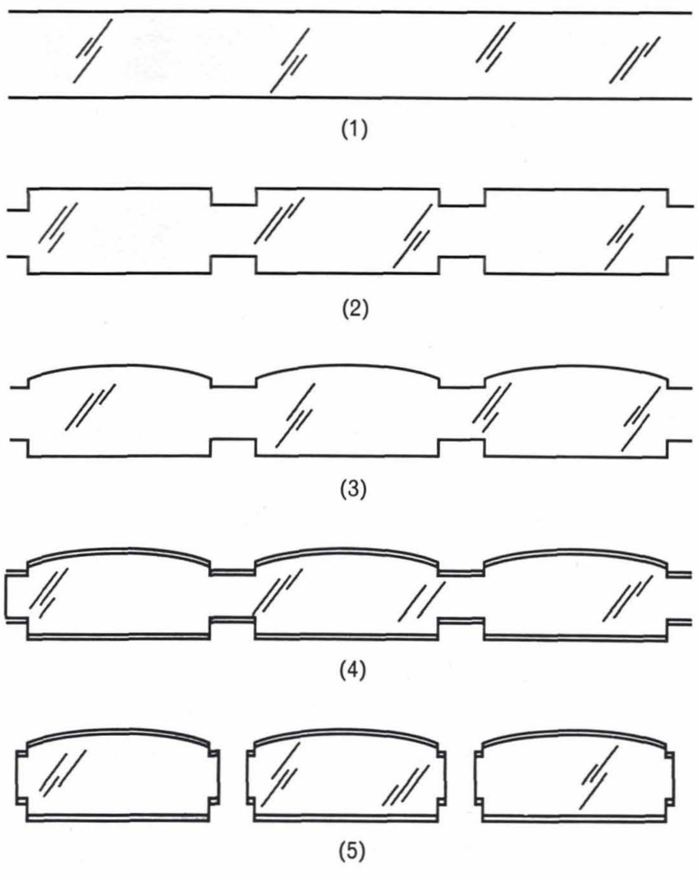

FIGURE A. Steps in fabricating an array of microchip lasers that have one flat mirror and one curved mirror. Cross section of (1) a wafer of gain medium polished flat and parallel, (2) a polished wafer scribed to define individual laser cavities, (3) a scribed wafer polished to produce curved surfaces, (4) a wafer dielectrically coated to create cavity mirrors, and (5) a wafer cut into individual microchip lasers.

Microchip lasers with curved mirrors can be inexpensively mass produced with a five-step process [1]:

1. Wafers of gain media are cut to the desired thickness and polished flat and parallel, as illustrated in Figure A(1). (The thickness of the wafer corresponds to the cavity length of the laser.)
2. The polished wafer is scribed in a grid pattern on one or both surfaces (Figure A[2]). The width and depth of the scribe must be sufficient to allow for the flow of the polishing slurry used in step 3. The distance between the scribe marks defines the transverse dimensions of the laser cavity.
3. The scribed wafer is again polished. During the polishing a natural rounding of the surface occurs, as shown in Figure A(3). The rounding results

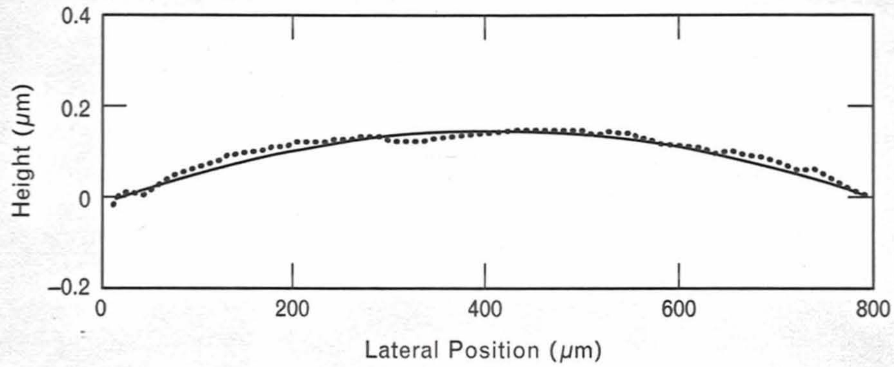

FIGURE B. Measured profile (dotted line) and ideal profile (solid line) of a mirror with a 50-cm radius of curvature.

from the deformation of the polisher surface and the build-up of slurry under the edges of each element. Several factors that determine the degree of rounding include the type of polisher used on the crystal during polishing, the type of slurry used, the width of the scribe, the amount of force applied to the crystal, and the polishing time. Each of these factors can be controlled to produce the desired amount of curvature.

4. The wafer is dielectrically coated (Figure A[4]) to create the proper-reflectivity cavity mirrors.
5. The wafer is cut along the center of the scribed channels to create the individual laser cavities (Figure A[5]). Cutting along the center of the scribed channels minimizes the amount of surface distortion that occurs when surface strains are relieved during cutting.

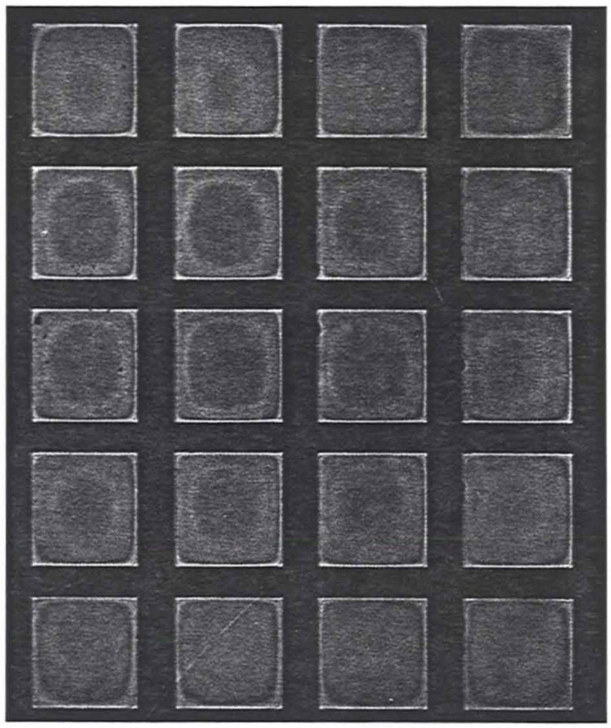

FIGURE C. Interferogram of an array of curved-mirror microchip lasers.

Using the procedure outlined above, we fabricated arrays of microchip lasers that had one flat mirror and one curved mirror. The curved mirrors had radii of curvature that ranged from 50 cm to 4 m. The deviations of the fabricated curved surfaces from ideal surfaces were less than $\lambda/50$, where $\lambda = 1.064$ μm. Figure B shows a profile that was taken through the center of a surface that had a 50-cm radius of curvature. Figure C shows an array of such devices.

References

1. J.J. Zayhowski and J.L. Daneu, "Technique for Mass Producing Two-Dimensional Arrays of Monolithic Solid State Laser Cavities with Curved Mirrors," *Solid State Research Report*, Lincoln Laboratory, pp. 23–28 (1990:2).

fundamental-transverse-mode operation is easily obtained. (See the box "Fundamental-Transverse-Mode Operation of Microchip Lasers" on p. 434.)

Because microchip lasers operate in a single longitudinal and transverse mode, the two orthogonal polarization modes of the cavity are perfectly correlated and effectively compete with each other for gain. The first mode to oscillate depletes the gain for the second mode, which never reaches threshold. In materials with cubic symmetry (such as Nd:YAG, a neodymium-doped garnet comprised of yttrium, aluminum, and oxygen), in which the two orthogonal modes are degenerate, the degeneracy can be broken with the application of uniaxial stress transverse to the cavity axis. Such stress decreases the lasing threshold for one of the polarizations relative to the other, and fixes the polarization of the laser.

Performance of Microchip Lasers

Microchip lasers have been fabricated from several different gain media, including Nd:YAG ($Nd_xY_{3-x}Al_5O_{12}$), Nd pentaphosphate (NdP_5O_{14}), LNP ($LiNdP_4O_{12}$), and Nd:GSGG ($Nd_xGd_{3-x}Sc_2Ga_3O_{12}$) [1, 2]. For each of these media, single-frequency, fundamental-transverse-mode operation was achieved with pump powers well above threshold. By far the most studied microchip lasers have been those fabricated from Nd:YAG and LNP. This section reviews the CW performance of these lasers.

Ti:Al_2O_3-Pumped Microchip Lasers

We used a Ti:Al_2O_3 laser as a pump source to characterize the microchip lasers prior to diode pumping. The Ti:Al_2O_3 laser was tuned to the Nd absorption peak near 808 nm and focused to an experimentally determined spot size of ~50 μm in the gain crystals. Table 1 on p. 436 summarizes the typical operating characteristics of several Ti:Al_2O_3-pumped microchip lasers [1, 2].

It should be noted that the maximum single-frequency output from a microchip laser is a strong function of the output coupler. Increasing the output coupling can increase the maximum single-frequency output well beyond the values shown in Table 1 (see the box "Single-Frequency Operation of Microchip Lasers"). Indeed, data from our preliminary high-power experiments indicate that single-frequency outputs in excess of 1 W are obtainable.

The far-field patterns of Ti:Al_2O_3-pumped microchip lasers are circularly symmetric and almost perfectly Gaussian, as illustrated in Figure 3, which shows data from a Nd:YAG device with an operating wavelength of 1.064 μm. The divergence of the beam varies with pump intensity (as discussed in the box "Fundamental-Transverse-Mode Operation of Microchip Lasers" on p. 434), but is typically 2 to 3 mrad. The output beam is polarized to better than 1 part in 10^4. (Our polarization measurements were instrument limited.)

We measured the linewidth of the 1.064-μm Nd:YAG microchip lasers by heterodyning two free-running devices. The output of a single Ti:Al_2O_3 laser was split and used to pump both devices. Thermal tuning was used to make the lasers operate at nearly the same frequency. The outputs of the lasers were stable enough for us to obtain heterodyne measurements with a resolution of 10 kHz as shown in Figure 4. At this resolution, the measured spectral response, which was instrument limited, corresponded to a maximum linewidth of less than 7 kHz. (The 7-kHz value assumes that each laser contributed equally to the measured linewidth.) Attempts to fit the heterodyne spectra to a Lorentzian lineshape gave a linewidth of only a few hertz (see the box "Fundamental Linewidth of Microchip Lasers" on p. 438). Heterodyne measurements performed with 1.32-μm Nd:YAG microchip lasers produced similar results, indicating that these devices also had a linewidth of less than 7 kHz.

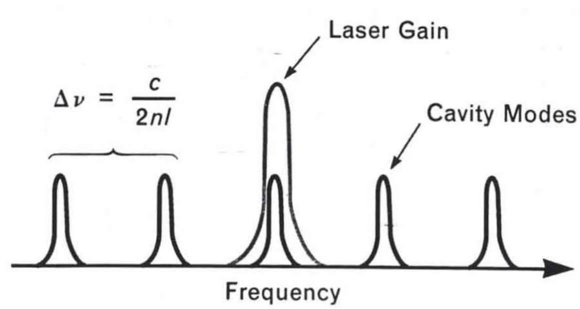

FIGURE 2. Gain spectrum of a hypothetical gain medium, with the resonances of a short cavity superimposed. The cavity length *l* has been chosen so that the mode spacing $\Delta\nu$ is greater than the bandwidth of the gain spectrum and so that one of the resonances falls at the frequency of maximum gain. The variable *n* is the index of refraction within the cavity and *c* is the speed of light in a vacuum.

SINGLE-FREQUENCY OPERATION OF MICROCHIP LASERS

MICROCHIP LASERS ARE pumped optically and longitudinally. Thus there is a limit on how short the laser cavity can be. If the cavity is made much shorter than the absorption length of the gain medium at the pump frequency, very little pump power will be absorbed. As a result, it is often not practical to make the cavity short enough so that only one cavity mode falls within the gain bandwidth of the laser. The situation is further complicated because most gain media have several gain peaks, as illustrated in Figure A, which shows the gain spectrum of Nd:YAG near 1.064 μm. Superimposed on the gain spectrum are the cavity modes of a 648-μm-long Nd:YAG cavity. This cavity length is already shorter than the absorption length at the peak of the Nd:YAG absorption profile.

To determine how much single-frequency output power can be obtained from a microchip laser, we must account for *spatial hole burning* and *energy diffusion* [1, 2]. In standing-wave laser cavities, such as the microchip cavity, the optical intensity of the first cavity mode to oscillate varies sinusoidally along the cavity axis, producing a pattern of peaks and nulls. At the peak positions the optical gain is partially depleted. At the nulls, on the other hand, the first mode to lase is unable to deplete the gain. This phenomenon is known as spatial hole burning. The gain at these nulls will eventually contribute to the lasing of a second cavity mode.

Spatial hole burning can be mediated by energy diffusion, which moves some of the gain away from the optical-field nulls toward the peaks, where it can be effectively depleted. A theoretical analysis shows that single-mode operation of a laser can be expected at pump powers up to $\zeta(1, 2)$ times the threshold pump power, where the integers 1 and 2 refer to the first and second modes to lase. The quantity $\zeta(1, 2)$ is given by the larger of

$$\zeta_{SH}(1,2) \equiv \left(\frac{\beta(1,2)-1}{1-\langle \psi(1,2)\rangle} + 1 \right) \times \left(\frac{2[\beta(1,2)-1]}{1-\langle \psi(1,2)\rangle} + 1 \right), \quad \text{(A)}$$

the pump ratio due to spatial hole burning, and

$$\zeta_D(1,2) \equiv (4k_1^{\,2} D\tau_{\text{eff}} - 1) \times \left(\frac{\beta(1,2)-1}{1-\langle \psi(1,2)\rangle} \right) \quad \text{(B)}$$

$$+4k_1^{\,2} D\,\tau_{\text{eff}} \left(\frac{\beta(1,2)-1}{1-\langle \psi(1,2)\rangle} \right)^2,$$

the pump ratio in the presence of energy diffusion.

In Equations A and B, k_1 is the magnitude of the wave vector of the first cavity mode to lase, D is the energy diffusion coefficient, τ_{eff} is the relaxation time for the gain in the absence of stimulated emission, $\beta(1, 2)$ is the discrimination factor, and $\langle \psi(1, 2)\rangle$ is the correlation fac-

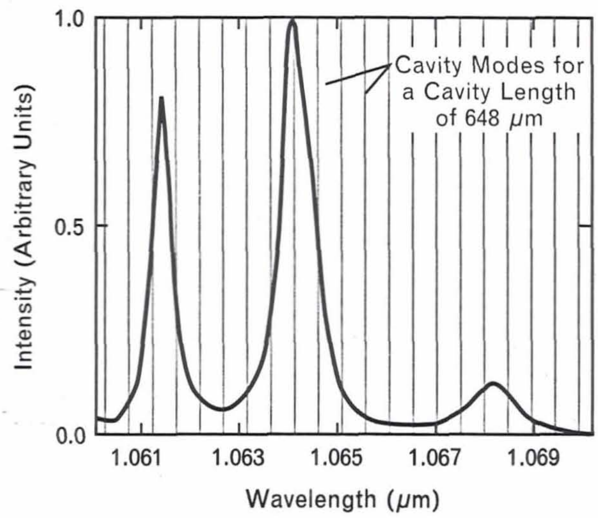

FIGURE A. Gain spectrum of Nd:YAG. The cavity-mode resonances of a Nd:YAG cavity that is 648 μm long are superimposed. Note that the cavity length was chosen so that a resonance falls at the maximum of the gain spectrum (λ = 1.064 μm) while other resonances straddle the secondary gain peak (λ = 1.0615 μm).

tor. The discrimination factor $\beta(1,2)$ is given by

$$\beta(1,2) \equiv \frac{\sigma_1 \gamma_2}{\sigma_2 \gamma_1}, \qquad \text{(C)}$$

where $\sigma_{1(2)}$ is the value of the emission cross section at the frequency corresponding to the first (second) mode to lase and $\gamma_{1(2)}$ is the total round-trip loss for the mode, including transmission through the cavity mirrors. For a microchip laser, the correlation factor $\langle \psi(1,2) \rangle$ is given by

$$\langle \psi(1,2) \rangle = \frac{1}{1+\left(\dfrac{2\pi \Delta m}{\alpha l}\right)^2}, \qquad \text{(D)}$$

where l is the cavity length, α is the absorption coefficient at the pump wavelength, and Δm is the difference in the longitudinal-mode numbers of the first and second modes to lase. Figure B shows $\zeta(1,2)$ as a function of $[\beta(1,2)-1]/[1-\langle \psi(1,2)\rangle]$ for several values of $4k_1^{\,2} D\tau_{\text{eff}}$. (Note that $\beta(1, 2)$ and $\langle \psi(1,2) \rangle$ appear only in the combination $[\beta(1,2)-1]/[1-\langle \psi(1,2)\rangle]$ in both Equations A and B.)

The pump ratio $\zeta(1,2)$ is a strong function of cavity length. To illustrate this point, consider a microchip laser that is operating on the 1.32-μm transition in Nd:YAG. Let one of the mirrors, the pump mirror, be highly reflecting at all potential lasing frequencies (reflectivity > 99.9%) and highly transmitting at the pump wavelength. Let the other mirror, the output coupler, have a reflectivity that is flat over the gain peak at 1.32 μm and greatly reduced at

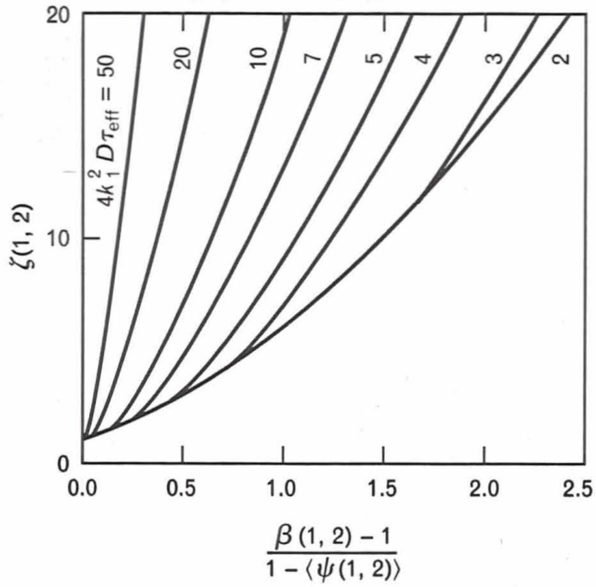

FIGURE B. Plot of $\zeta(1, 2)$, the maximum pump ratio for single-frequency operation, as a function of $[\beta(1, 2) - 1]/[1 - \langle \psi(1, 2)\rangle]$, where $\beta(1, 2)$ is the discrimination factor given by Equation C and $\langle \psi(1, 2)\rangle$ is the correlation factor given by Equation D. The different curves represent different values of $4k_1^{\,2} D\tau_{\text{eff}}$, where k_1 is the magnitude of the wave vector of the first cavity mode to lase, D is the energy diffusion coefficient, and τ_{eff} is the relaxation time for the gain in the absence of stimulated emission.

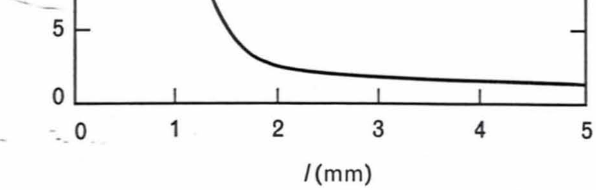

FIGURE C. Plot of $\zeta(1, 2)$, the maximum pump ratio for single-frequency operation, as a function of cavity length l for a 1.32-μm Nd:YAG microchip laser (see insert). The figure assumes that $4k_1^{\,2} D\tau_{\text{eff}} = 5$, where k_1 is the magnitude of the wave vector of the first cavity mode to lase, D is the energy diffusion coefficient, and τ_{eff} is the relaxation time for the gain in the absence of stimulated emission.

all other gain peaks, so that only the 1.32-μm peak needs to be considered. At room temperature, the 1.32-μm gain peak can be approximated as Lorentzian, with a half-width λ_{half} of 0.4 nm. To complete the definition of the problem, the laser is longitudinally pumped through the pump mirror with a diode laser at 808 nm. We will assume that the Nd concentration is such that the absorption length for the pump is 1 mm, and we will neglect any reflection of the pump light by the output coupler. The question we will ask is, how does the maximum single-mode output power change as the cavity length is changed?

To simplify the analysis we will change the cavity length discretely, such that one of the cavity modes always falls at the peak of the gain profile. This mode will always be the first mode to lase. (In practice, to do this would require interferometric control of the cavity length.) The discrimination factor $\beta(1,2)$ is given by the inverse of the Lorentzian line shape:

$$\beta(1,2) = 1 + \left[\frac{\Delta\lambda(1,2)}{\lambda_{\text{half}}}\right]^2, \quad \text{(E)}$$

where $\Delta\lambda(1,2)$ is the difference in wavelength between the first mode to oscillate and a potential second mode. The value of $\Delta\lambda(1,2)$ is given by the equation

$$\Delta\lambda(1,2) = \frac{\Delta m\lambda_0^{\,2}}{2nl}, \quad \text{(F)}$$

in which λ_0 is the wavelength at the gain peak (λ_0 = 1.32 μm), and n is the refractive index within the cavity (n = 1.8). Equations D, E, and F lead to the following expression:

$$\frac{\beta(1,2)-1}{1-\langle\psi(1,2)\rangle} = \frac{\left(\alpha l\lambda_0^2\right)^2 + \left(2\pi\Delta m\lambda_0^2\right)^2}{\left(4\pi\lambda_{\text{half}}nl\right)^2}.$$

The smallest value of the pump ratio $\zeta(1,2)$ corresponds to $\Delta m = 1$ for all cavity lengths, and is plotted as a function of cavity length in Figure C for a value of D such that $4k_1^{\,2}D\tau_{\text{eff}} = 5$.

References

1. J.J. Zayhowski, "Limits Imposed by Spatial Hole Burning on the Single-Mode Operation of Standing-Wave Laser Cavities," *Opt. Lett.* **15**, 431 (1990).
2. J.J. Zayhowski, "Effects of Spatial Hole Burning and Energy Diffusion on the Single-Mode Operation of Standing-Wave Lasers," *IEEE J. Quantum Electron.* (to be published in Dec. 1990).

Figure 4 shows the heterodyne spectrum of two 1.064-μm Nd:YAG microchip lasers. Relaxation oscillations account for the observed sidebands 700 kHz away from the main peak (Figure 4[a]). At higher pump powers these sidebands were moved to greater than 1 MHz away from the main peak. The intensity of the sidebands varied with time, but was always greater than 30 dB below the main peak. The magnitude of the relaxation sidebands should decrease with increased stability of the pump source, as can be obtained with diode pumping.

Diode-Pumped Microchip Lasers

Microchip lasers have also been pumped with the unfocused output of GaAlAs diode lasers operating at a wavelength of 808 nm. The microchip cavity is placed in front of the output facet of the diode laser and is longitudinally pumped. The performance of diode-pumped microchip lasers is similar to the performance of Ti:Al_2O_3-pumped devices, with only slight differences. As a result of the noncircular intensity profile of the pump, the far-field profile of a diode-pumped microchip laser is slightly elliptical, as shown in Figure 5. However, the divergence of the output beam remains diffraction limited, and is still typically ~2 mrad. Since the diode pump spot tends to be larger than the Ti:Al_2O_3 pump spot, the operating threshold of diode-pumped devices is slightly higher. The slope efficiencies are about the same.

As an example, we pumped a 1.32-μm Nd:YAG microchip laser with a 480-mW diode laser. The microchip laser absorbed 60% of the incident pump power and had a lasing threshold of approximately 75 mW of absorbed power. The output showed single-frequency, fundamental-transverse-mode operation at all available diode pump powers, and was polarized to better than 1 part in 10^4. The maximum CW output power obtained was 51 mW, the slope optical quantum efficiency was greater than 40%, and the overall wall-socket efficiency (i.e., the ratio of electrical input to 1.32-μm optical output) was greater than 4%. Attempts to measure

FUNDAMENTAL-TRANSVERSE-MODE OPERATION OF MICROCHIP LASERS

IN A MICROCHIP LASER the heat deposited by the pump beam diffuses in an outward direction from the cavity axis. In materials such as Nd:YAG that have a positive dn/dT, in which n is refractive index and T is temperature, this distribution results in a thermal waveguide. With such a material, it can be shown [1] that in flat-flat cavities a Gaussian pump beam results in a nearly Gaussian fundamental guided mode whose waist size ω_0 is given by

$$\omega_0^2 = \lambda \left[\frac{(r_0^2 + r_P^2)lk}{Q_P \pi \left(n_0 \dfrac{dn}{dT} \right)} \right]^{\frac{1}{2}}, \quad \text{(A)}$$

where r_P is the radius of the pump, Q_P is the amount of heat deposited by the pump, λ is the lasing wavelength, l is the cavity length, k is the thermal conductivity of the gain medium, n_0 is the refractive index in the absence of thermal effects, and dn/dT is the linear change in refractive index with temperature (determined experimentally). The value of r_0 is obtained by measuring the value of ω_0 for a tightly focused pump and solving Equation A.

For a Nd:YAG microchip laser operating at 1.064 μm, experimental values of ω_0 are plotted as a function of pump power and pump radius in Figures A and B, respectively. The figures also show curves that correspond to the fit of Equation A.

It is important to note that as long as the radius of the pump spot is kept smaller than the waist of the fundamental guided mode, only the fundamental transverse mode will be excited. For Nd:YAG microchip lasers the properties of the gain medium are such that the waist size of the fundamental mode is larger than the pump field produced by an unfocused, tight-coupled diode laser.

For the microchip laser to oscillate in a well-defined transverse mode the two cavity mirrors must

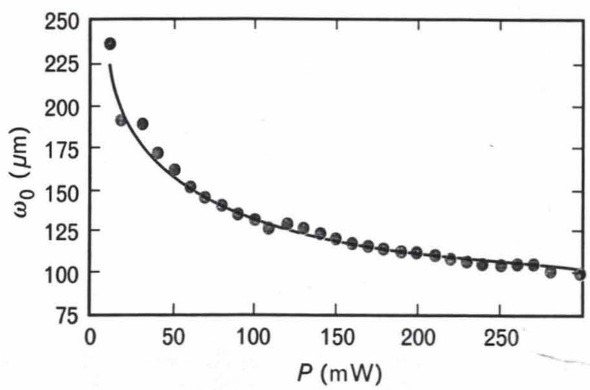

FIGURE A. Beam waist size ω_0 of the fundamental transverse mode of a microchip laser as a function of incident pump power P for a pump focused to a 17-μm radius. The plotted points represent experimental data; the curve corresponds to the equation $\omega_0^2 = 5986/\sqrt{P}\ \mu\text{m}^2$, with P in watts.

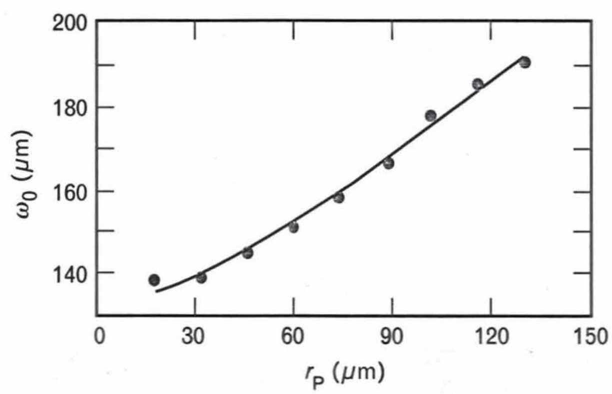

FIGURE B. Beam waist size ω_0 of the fundamental transverse mode of a microchip laser as a function of the radius of the pump spot r_P for 100 mW of incident pump power. The plotted points represent experimental data; the curve corresponds to the equation $\omega_0^2 = 241(75^2 + r_P^2)^{1/2} \mu\text{m}^2$, with r_P in microns.

the linewidth were instrument limited, corresponding to a maximum linewidth of 7 kHz. The linewidth determined from a Lorentzian fit to the heterodyne measurements was less than 300 Hz (see the box "Fundamental Linewidth of Microchip Lasers" on p. 438), and the relaxation sidebands were suppressed by more

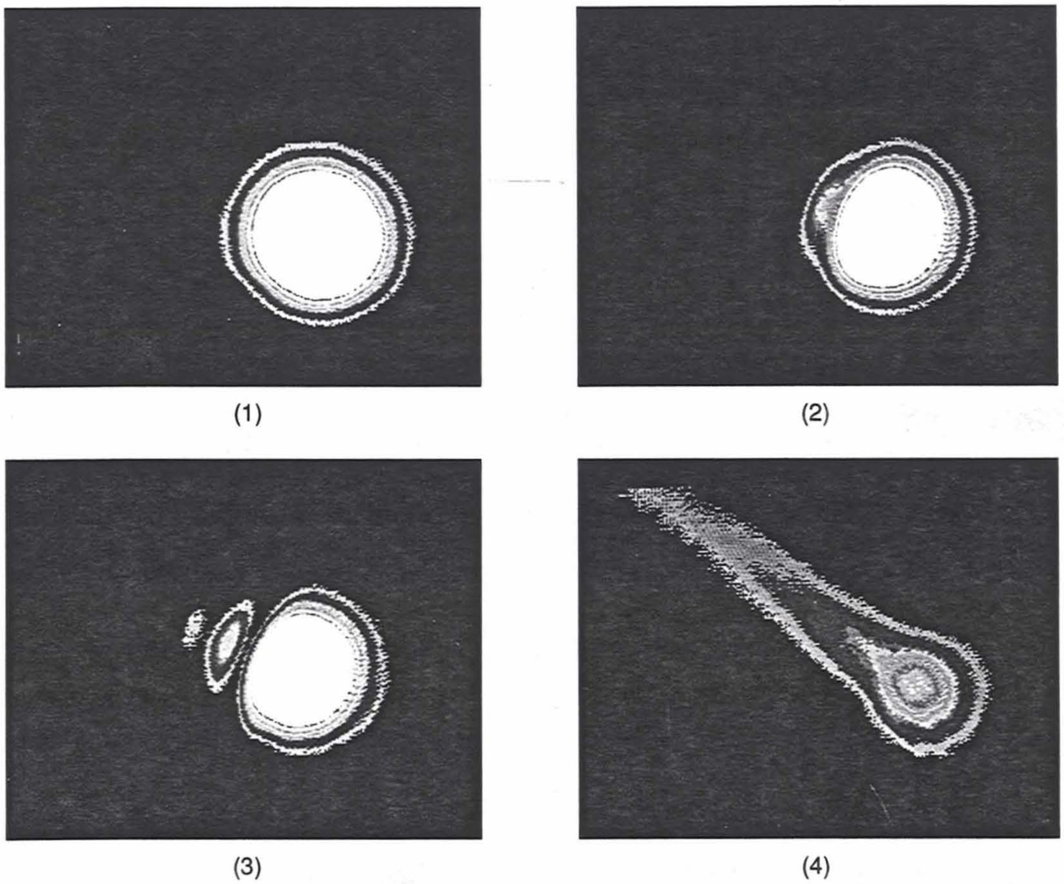

FIGURE C. False-color images of the far-field profiles of a misaligned microchip laser. The incident pump power was 300 mW focused to a 17-μm radius at the pump surface of the microchip laser, giving an angular tolerance in mirror misalignment $\Delta\psi_{max} \sim 3.3 \times 10^{-5}$ radians. The images are for increasing values of angular misalignment of the microchip mirrors: (1) 3.3×10^{-5} radians, (2) 3.6×10^{-5} radians, (3) 4.2×10^{-5} radians, and (4) 9.2×10^{-5} radians. Large areas of white in the figures correspond to saturation of the charge-injection-device camera.

be very nearly parallel. The angular tolerance in mirror misalignment $\Delta\psi_{max}$ is determined by the strength of the thermally induced waveguide, and can be shown [1] to be given by

$$\Delta\psi_{max} \approx \frac{1}{k}\left(\frac{Q_P}{4\pi r_P}\right)\frac{dn}{dT}.$$

For larger amounts of mirror misalignment the far-field intensity pattern of the microchip laser begins to develop a sidelobe (Figure C). With increasing mirror misalignment, the sidelobe evolves into a continuous tail that resembles the tail of a comet, as shown in Figure C(4).

References

1. J.J. Zayhowski, "Thermal Guiding in Microchip Lasers," in *OSA Proceedings on Advanced Solid State Lasers*, eds. G. Dubé and H.P. Jenssen (Optical Society of America, Washington, DC, 1990), to be published.

than 40 dB. We found that the thermal and mechanical stability of the microchip package determined the frequency stability of the laser. In a thermally stabilized and mechanically isolated environment, the measured frequency drift was less than 250 kHz over a 1-sec period and less than 3 MHz over a 10-min period.

Piezoelectric Tuning of Microchip Lasers

Because of the extremely short cavity lengths l of microchip lasers, a small change in length δl results in a relatively large frequency shift $\delta\nu$ away from the initial operating frequency ν_0; i.e., $\delta\nu = \nu_0 \delta l / l_0$. A 1.064-$\mu$m Nd:YAG microchip laser with a 750-μm long cavity tunes

Table 1. Characteristics of Several $Ti{:}Al_2O_3$-Laser-Pumped Microchip Lasers

	Gain Medium		
	$Nd_xY_{3-x}Al_5O_{12}$	$Nd_xY_{3-x}Al_5O_{12}$	$LiNdP_4O_{12}$
Cavity Characteristics			
Output coupler (%)	0.3	1.0	1.3
Cavity length (μm)	730	1000	140
Operating wavelength (μm)	1.064	1.319	1.048
Performance Characteristics			
Single-frequency output power (mW)	22	100*	26*
Slope quantum efficiency (%)	46	44	28
Threshold (mW absorbed)	0.7	13	3.4
Pump power absorbed (%)	55	86	65

*Output power was limited by the available pump power

at a rate of 400 MHz per nm of cavity-length change. Thus, by applying a transverse stress to a small, monolithic Nd:YAG laser, we can change the laser's length enough to tune the device over a large portion of its gain bandwidth [2–4].

The microchip lasers discussed in this section were fabricated from a piece of Nd:YAG that was cut and polished to a thickness of 650 μm. The output mirror had a reflectivity of 99.7% at a lasing wavelength of 1.064 μm and reflected the pump laser. The opposite mirror had a reflectivity of 99.9% at 1.064 μm and transmitted the pump. To enable the dynamic tuning of a microchip laser, we cut the Nd:YAG into a 1 × 2-mm piece and fitted it tightly into a U-shaped beryllium-copper holder adjacent to a lead zirconate-titanate (PZT) piezoelectric transducer, as shown in Figure 6. To tune the microchip laser, a voltage is applied to the piezoelectric transducer, which then applies stress to the Nd:YAG laser in a direction orthogonal to the laser cavity, causing the cavity length to change. In these experiments, we observed single-frequency, single-polarization, fundamental-transverse-mode opera-

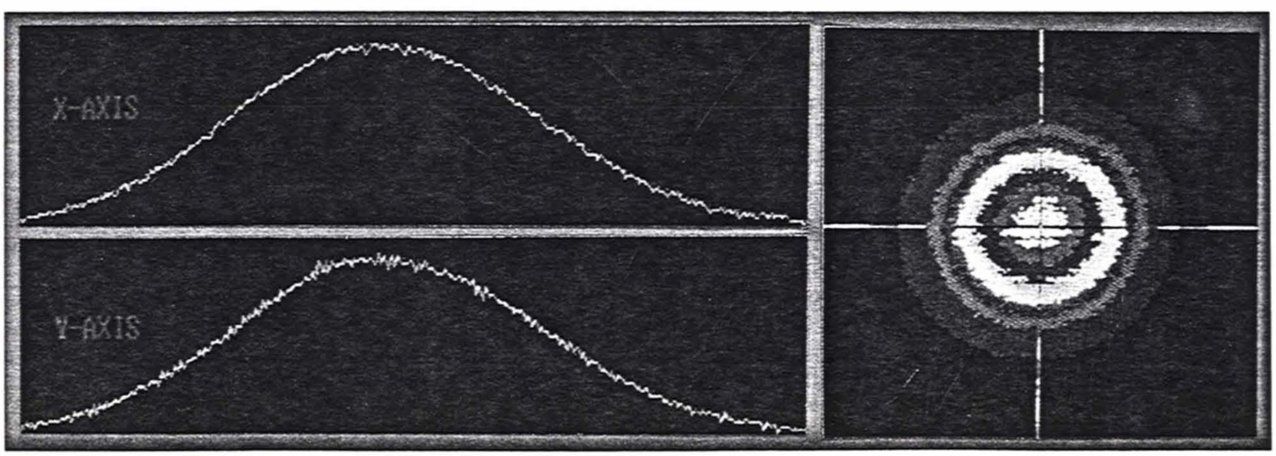

FIGURE 3. Far-field intensity profile of a microchip laser pumped by a $Ti{:}Al_2O_3$ laser. The right portion of the figure shows the image obtained by mapping the two-dimensional field intensity into different colors. The left portion shows an almost perfectly Gaussian intensity profile in two orthogonal directions.

tion over the entire stress-tuning range.

Figure 7 shows several spectra obtained by heterodyning the above tunable microchip laser with a fixed-frequency device. Figure 7(a) shows an instrument-limited linewidth of less than 7 kHz for the microchip laser with zero voltage applied to the piezoelectric transducer. The data in Figure 7(b) were obtained by piezoelectrically driving the laser with a ±800-V sine wave at 1 kHz. The spectrum deviated from the expected theoretical curve (note the slight hump in the middle of the figure) due to the heterodyne system's frequency response, which was not flat over the entire range. Similar spectra over a smaller tuning range, in which the spectral response of the detection system was relatively flat, were in excellent agreement with calculations (Figure 8) if we assume that the output frequency of the tunable laser varied linearly with applied voltage. Experimentally, the tuning response for the 1.064-μm Nd:YAG microchip lasers discussed here was measured to be 0.3 MHz/V for applied voltages between −1000 and 1000 V (the largest voltages used in these experiments) and was constant for modulation frequencies from dc to 80 kHz.

At modulation frequencies greater than 80 kHz the tuning response of the microchip lasers was dominated by mechanical resonances of the microchip-transducer-holder system. Specifically, at resonant frequencies between 80 kHz and 1.0 MHz the tuning was typically enhanced by a factor of 5. At a modulation frequency of approximately 1.1 MHz we observed a very strong resonance that enhanced the tuning response by a factor of 44, to 13.2 MHz/V. This resonance was identified as a fundamental acoustic resonance of the Nd:YAG crystal. Figures 7(c) and 7(d) show the heterodyne spectra obtained when the microchip laser was modulated at rates corresponding to its mechanical resonances at 5 and 19 MHz.

In a more recent design of the piezoelectrically tunable microchip-laser package, it was possible to increase the maximum flat-band tuning rate from 80 kHz to 300 kHz before the mechanical resonances of the package were reached. At the same time, the tuning response was increased to 0.6 MHz/V. Further improvements are still possible.

As an alternative to piezoelectric tuning, electro-optically tuned microchip lasers are currently being built. With electro-optic tuning, it should be possible to obtain a flat-band tuning response in excess of 10 MHz/V

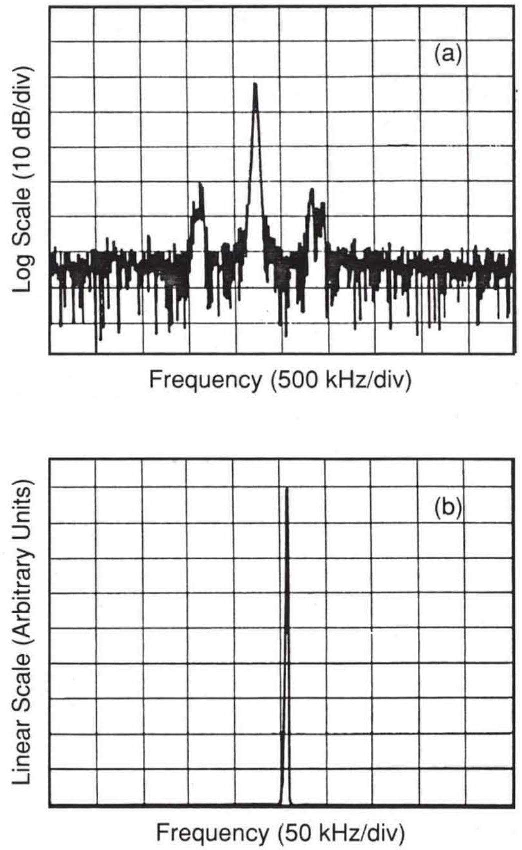

FIGURE 4. Instrument-limited heterodyne spectrum of two CW 1.064-μm Nd:YAG microchip lasers: (a) on a logarithmic scale, and (b) on an expanded horizontal scale and vertical linear scale. The resolution bandwidth for both figures is 10 kHz.

at rates up to several gigahertz, and a tuning range limited by the free spectral range of the laser cavity [5].

Pulsed Operation of Microchip Lasers

The short cavity lengths of microchip lasers result in very short cavity lifetimes and the possibility of gain-switched pulses (pulses obtained by quickly changing the intensity of the pump) and Q-switched pulses (pulses obtained by quickly changing the quality, or *Q*, of the cavity) that are much shorter than can be obtained with more conventional solid state lasers. Both gain-switched and Q-switched microchip lasers have been demonstrated.

Gain-Switched Microchip Lasers

Using Nd:YAG microchip lasers, we have produced single-frequency gain-switched pulses with a temporal full width at half maximum (FWHM) as short as 760 psec and peak powers of more than 1 kW [6]. To

FUNDAMENTAL LINEWIDTH OF MICROCHIP LASERS

ONE CONTRIBUTION to the finite spectral width of all lasers is the coupling of spontaneous emission to the oscillating mode [1, 2]. This contribution, which A.L. Schawlow and C.H. Townes [1] originally described, results in a Lorentzian power spectrum. For many lasers, this contribution alone determines the fundamental linewidth, and it is common practice to determine the fundamental linewidth of a laser by fitting the tails of the measured power spectrum to a Lorentzian curve.

In microchip lasers, there is a second important contribution to the fundamental linewidth—the thermal fluctuations of the cavity length at a constant temperature. This contribution is expected to result in a Gaussian power spectrum. Because of the short cavity length of microchip lasers, the contribution due to thermal fluctuations is much larger than that due to spontaneous emission. Since a Gaussian curve decays much more quickly than a Lorentzian curve, however, the tails of the power spectrum will still correspond to the Lorentzian contribution. Therefore, it is important to understand both the effects of spontaneous emission and thermal fluctuations.

The Lorentzian contribution to the fundamental linewidth of a microchip laser has a full width at half maximum (FWHM) that is given by the equation

$$\Delta\nu_L = \frac{h\nu_0}{16\pi P_O}\left(\frac{c}{nl}\right)^2 \times \left[\ln R - 2\alpha_L l\right]\ln R, \qquad \text{(A)}$$

where

h = Planck's constant,

ν_0 = the center frequency of the laser,

P_O = the output power,

c = the speed of light in a vacuum,

n = the refractive index,

l = the cavity length,

R = the reflectivity of the output coupler, and

α_L = the roundtrip cavity loss not including transmission through the output coupler.

For microchip lasers, $\Delta\nu_L$ from Equation A is typically a few hertz, which is consistent with experimental measurements.

We can easily calculate the spectral-broadening effects of thermal fluctuations in cavity length by using the principle of *equipartition of energy.* This principle, derived from classical mechanics, states that whenever the energy of a system can be written as a sum of independent terms, each of which is quadratic in the variable that represents the associated degree of freedom, then the following will apply: when the system is in equilibrium at temperature T, each of the terms (i.e., each degree of freedom) will contribute $k_B T/2$ to the energy of the system, where k_B is Boltzmann's constant. For the microchip laser, the principle of equipartition of energy leads to the expression

$$C_{11}\left\langle\left(\frac{\Delta l}{l}\right)^2\right\rangle V = k_B T, \qquad \text{(B)}$$

where C_{11} is the longitudinal elastic constant, Δl is the change in the cavity length l, V is the volume of the lasing mode, and the angle brackets indicate an averaging over time. Equation B results in a Gaussian contribution to the fundamental linewidth, with a FWHM of

$$\Delta\nu_G = \nu_0\left(\frac{8k_B T\ln 2}{C_{11}V}\right)^{\frac{1}{2}}.$$

For microchip lasers the value of $\Delta\nu_G$ varies with pump power and pump-beam diameter (see the box "Fundamental-Transverse-Mode Operation of Microchip Lasers" on p. 434). Under the conditions of our heterodyne measurements, $\Delta\nu_G$ is typically between 5 and 7 kHz, which is comparable to our instrument resolution.

Other factors that contribute to the linewidth of the microchip laser include amplitude and frequency fluctuations of the pump beam (different frequencies of light experience different absorption coefficients in the Nd:YAG material), optical feedback into the microchip laser (including lasing light transmitted through the input mirror of the device and reflected back from the front facet of the butt-coupled diode laser pump), mechanical vibrations, and temperature variations. These contributions are less fundamental, however, and can be controlled. In addition, they tend to occur on a longer time scale than spontaneous emission and thermal fluctuations. Although these less fundamental contributions are probably not important in our attempts to measure the fundamental linewidth of microchip lasers, they are important in measurements of laser frequency stability on a longer time scale.

References

1. A.L. Schawlow and C.H. Townes, "Infrared and Optical Masers," *Phys. Rev.* **12**, 1940 (1958).
2. M. Lax, "Quantum Noise V: Phase Noise in a Homogeneously Broadened Maser," in *Physics of Quantum Electronics*, eds. P.L. Kelley, B. Lax, and P.E. Tannenwald (McGraw-Hill, New York, 1966) pp. 735–747.

our knowledge, these are the shortest gain-switched pulses obtained from a Nd:YAG laser. With LNP microchip lasers, we have obtained single-frequency gain-switched pulses as short as 80 psec [6]. In both cases, a gain-switched Ti:Al_2O_3 laser with a peak power of several kilowatts pumped the microchip lasers.

It is difficult for diode lasers to supply the high pump powers required to obtain subnanosecond pulses from gain-switched microchip lasers. Using a 500-mW diode laser pump, however, we were able to gain-switch a 1.32-μm Nd:YAG microchip laser to produce a 100-kHz train of 170-nsec pulses [7]. The microchip laser was constructed from 1.3-wt% Nd:YAG with a cavity length of 1 mm and a 1% output coupler. A Ge avalanche photodiode monitored the microchip-laser output.

Rate-equation analysis [6] indicates that the population-inversion density that can be obtained during the pulse buildup time largely determines the width of the output pulse generated in a gain-switched system. In order to obtain the maximum population inversion in the microchip laser, the pump laser should initially be biased below the lasing threshold of the microchip laser. The output of the pump should then be quickly increased to its maximum power and maintained at that level until the microchip pulse develops, whereupon the output should be quickly reduced to below the microchip-laser threshold to prevent the formation of a second pulse.

Experimentally, we obtained the above conditions by driving the diode laser pump with the superposition of a square wave and a dc component. The output of the microchip laser was monitored as the dc level and the frequency of the square wave were adjusted to obtain the

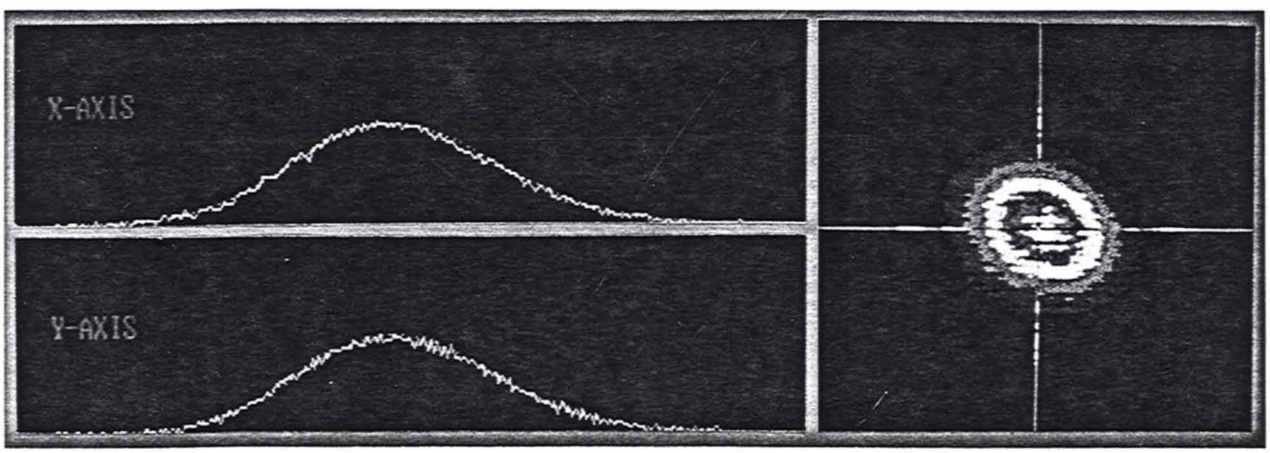

FIGURE 5. Far-field intensity profile of a diode-pumped 1.064-μm Nd:YAG microchip laser. The right portion of the figure shows the image obtained by mapping the two-dimensional field intensity into different colors. Note that the image is slightly elliptical, in contrast to the circular profile of Figure 3. The left portion shows an almost perfectly Gaussian intensity profile in two orthogonal directions.

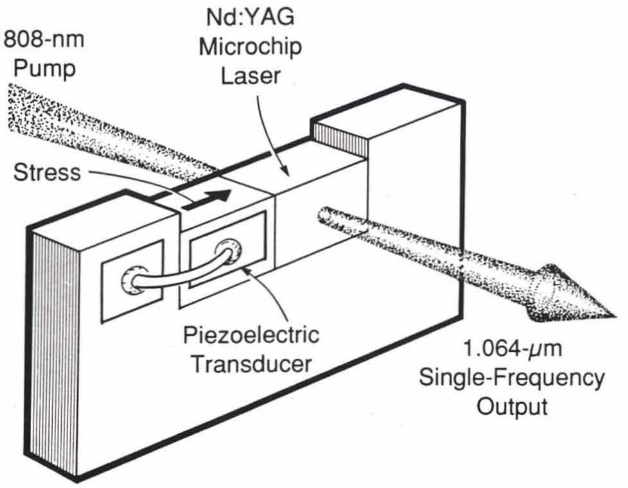

FIGURE 6. Piezoelectrically tunable, single-frequency Nd:YAG-microchip-laser package. The size of the Nd:YAG crystal used in the experiments was 0.65 × 1.0 × 2.0 mm.

narrowest pulses possible without any double pulses. The magnitude of the square wave was maintained so that the maximum output from the diode laser was 500 mW, the device's maximum rated power. This input resulted in a pump waveform that consisted of a 100-kHz, 400-mW (peak-to-peak) square wave superimposed on an average dc output power of 300 mW. During gain-switched operation, the microchip laser maintained single-frequency, single-polarization, fundamental-transverse-mode operation. Figure 9 shows the microchip output's temporal profile—a 100-kHz train of 170-nsec pulses. The long tail of the pulse shown in Figure 9(b) is an artifact of the detector. The measured average output power of the microchip laser was 30 mW; the peak output power was 1.8 W.

Q-Switched Microchip Lasers

Diode-laser-pumped pulsed operation of microchip lasers is also possible if the devices are CW-pumped and Q-switched after a sufficient population-inversion density is obtained. Computer modeling indicates that with a 500-mW diode laser pump it should be feasible to obtain Q-switched pulses with an FWHM of less than 250 psec and peak powers of several kilowatts from a Nd:YAG microchip laser. The computer model assumes that the Q of the laser cavity can be switched in a time that is short compared to the pulse buildup time and that the power efficiency of the Q-switched microchip laser is comparable to that of CW microchip lasers.

To realize a Q-switched microchip laser we use a novel Q-switching method that exploits the large cavity-mode spacing of the microchip laser. In this method, a tunable etalon (two surfaces that act like a Fabry-Perot interferometer) replaces the output coupler of a CW device. The reflectivity of the etalon at the lasing wavelength of the microchip laser (determined by the fixed optical distance between the pump mirror and the first of the two partially reflecting mirrors that form the tunable etalon) is a strong function of the etalon's optical length. By changing this length, we can switch the Q of the laser cavity. In the low-Q state, lasing is suppressed and the population inversion can become very large. If the free spectral range of the etalon is approximately the same as the mode spacing of the microchip laser, all potential lasing modes of the laser will see the same reflectivity and the suppression of one mode will not lead to a second mode's reaching threshold. Figure 10 illustrates this concept. A large population-inversion density results in a short output pulse when the laser cavity is switched to the high-Q state.

To demonstrate this technique, we constructed a Q-switched microchip laser from a CW 1.064-μm Nd:YAG microchip laser, a discrete flat partially reflecting mirror, and an annular piezoelectric actuator. The CW microchip laser consisted of a 650-μm-long piece of 1.3-wt% Nd:YAG with two flat mirrors (a pump mirror and a partially reflecting output mirror). The discrete partially reflecting mirror was mounted on the piezoelectric actuator and held parallel to the mirrors of the CW microchip laser as shown in Figure 11. The piezoelectric actuator had a nominal response of 0.5 μm/kV. The partially reflecting output mirror of the CW microchip laser, the discrete partially reflecting mirror, and the piezoelectric actuator formed the tunable etalon discussed above. To Q-switch the device, we changed the voltage applied to the piezoelectric actuator.

The Q-switched microchip laser was pumped with 120 mW of incident 808-nm light from a $Ti:Al_2O_3$ laser. (Note that this amount of pump power can be easily obtained from a diode laser.) We performed Q-switching by driving the piezoelectric actuator with the superposition of a dc component and a 100-V (peak-to-peak) triangular wave at a frequency of 40 kHz. We selected the dc component and the frequency of the triangular wave to give the minimum pulse width.

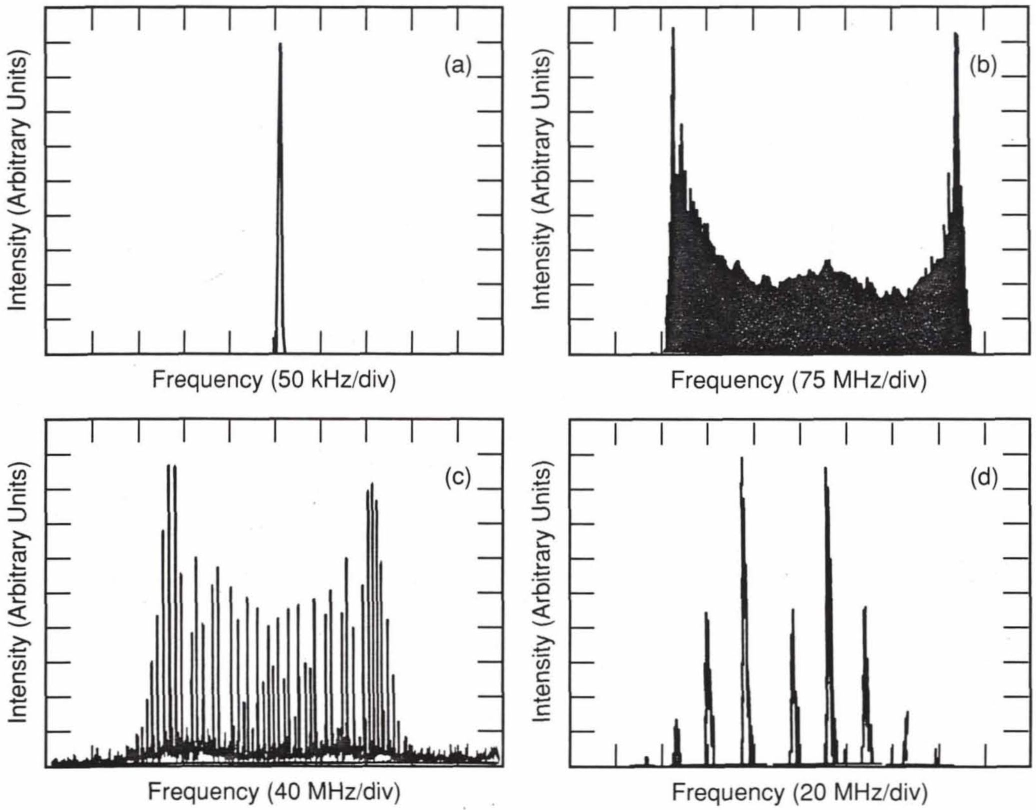

FIGURE 7. Spectra obtained by heterodyning two single-frequency 1.064-μm Nd:YAG microchip lasers; one of the lasers is piezoelectrically tunable and the other has a fixed frequency: (a) No voltage is applied to the transducer of the tunable laser. The resulting instrument-limited spectrum corresponds to a linewidth of less than 7 kHz for each laser. (b) The piezoelectrically tunable laser is driven by a ±800-V sine wave at ~1 kHz. The spectrum deviates from the expected theoretical curve (note the slight hump in the middle of the figure); the deviation is due to the heterodyne system's frequency response, which was not flat over the entire range. (c) The piezoelectrically tunable laser is driven by a ± 20-V sine wave at an acoustic resonance near 5 MHz. (d) The piezoelectrically tunable laser is driven by a ± 20-V sine wave at an acoustic resonance near 19 MHz.

The frequency and the slew rate of the voltage supply dictated the magnitude and shape of the ac component of the drive signal. During Q-switching the microchip laser maintained single-frequency, single-polarization, fundamental-transverse-mode operation. Two output pulses were produced during each drive period. As shown in Figure 12, the FWHM of the pulses was ~6 nsec, and we observed no afterpulsing. (These results are already among the shortest Q-switched pulses obtained from a Nd:YAG laser, and there is much room for improvement.) The pulse-to-pulse amplitude fluctuations were less than 5%. The averaged output power of this device was 3.5 mW; the peak output power was ~7 W. Most of the output (70%) was through the pump mirror.

The pump mirror of the CW microchip laser used in the Q-switched device transmitted the pump light and had a reflectivity of ~99.9% at 1.064 μm; the partially reflecting output mirror reflected the pump light and had a reflectivity of ~98.5% at the lasing wavelength. The discrete partially reflecting mirror had a reflectivity of ~99.7% at 1.064 μm. These high reflectivities resulted in most of the energy being lost within the laser cavity rather than being coupled to the output beam. A better choice of reflectivities for the partially reflecting mirrors should lead to power efficiencies of up to 33%, comparable to those obtained with CW microchip lasers, provided that the time between Q-switched pulses is shorter than the spontaneous relaxation time of the gain medium. Lower-reflectivity partially reflecting mirrors will also result in a shorter cavity lifetime, lead-

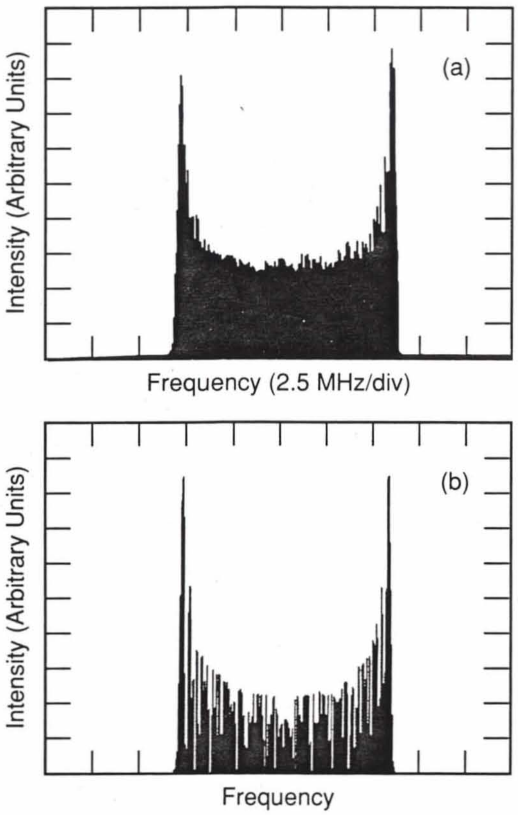

FIGURE 8. Piezoelectric tuning of a single-frequency Nd:YAG microchip laser: (a) heterodyne spectrum of a frequency-modulated laser driven by a ± 20-V sine wave at ~3 kHz, and (b) theoretical FM spectrum calculated for a peak frequency deviation of 160 times the modulation rate.

ing to shorter output pulses. Furthermore, with lower reflectivities most of the output power can be obtained through these mirrors instead of the pump mirror.

In future versions of the Q-switched microchip laser we intend to use an electro-optically tuned etalon bonded directly to the Nd:YAG, a diode laser pump, and a better choice of partially reflecting mirrors. An electro-optic etalon should allow quicker Q-switching of the laser and produce even shorter output pulses. The capability of a microchip laser to produce subnanosecond pulses with peak powers of several kilowatts could lead to applications in range finding and nonlinear optics.

Polarization-Switched Microchip Lasers

As a slight variation to the Q-switched microchip laser discussed in the previous subsection, we introduced a birefringent element between the two partially reflecting mirrors of the tunable etalon. Addition of the element caused the two orthogonal polarizations of the laser to see a low-Q cavity at different times as the tunable etalon was swept across its free spectral range. Application of the proper choice of voltages to the piezoelectric actuator allowed switching of the laser between the two polarizations.

The output of a polarization-switched microchip laser was split with a polarizing beam splitter and sent to two detectors. Both detectors had the same sensitivity, although one had a much faster response time. Each detector saw a different polarization of light from the laser. With the proper biasing of the piezoelectric actuator, a 200-V square wave superimposed on the actuator resulted in the complete switching of the laser's polarization, as shown in Figure 13. Using a fast photodetector (response time equal to 50 psec), we determined that the polarization switching took place in <50 μsec, as shown in Figure 14. This switching time was faster than

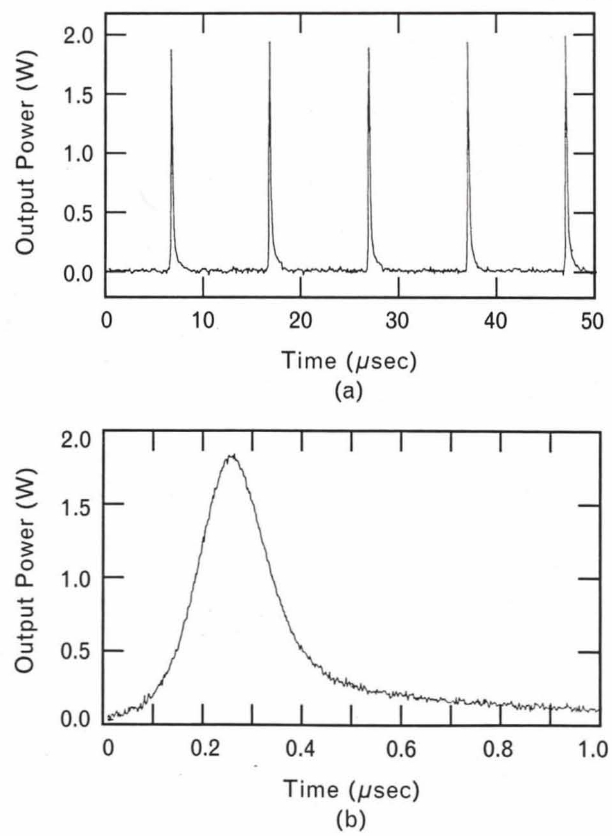

FIGURE 9. Output obtained from a 1.32-μm gain-switched diode-pumped Nd:YAG microchip laser: (a) train of pulses and (b) expanded time scale showing one pulse.

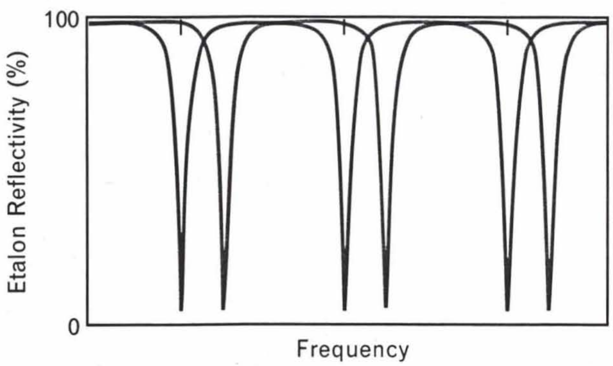

FIGURE 10. Reflectivity of an etalon as a function of frequency. The potential lasing wavelengths of a microchip laser are indicated by the tick marks at the top of the figure. For the device discussed in the text, they are spaced ~127 GHz apart. The length of the etalon has been chosen so that the free spectral range of the etalon is the same as the mode spacing of the microchip laser. The blue curve corresponds to the etalon tuned so that it is highly transmitting at the potential lasing frequencies of the microchip laser. The magenta curve corresponds to the etalon tuned so that it is highly reflecting.

the time required for the driving voltage to switch between its high and low state, indicating that the slew rate of the driving voltage might have been a limiting factor. There was no relaxation spiking (i.e., intensity spiking of the laser output that results from a sudden change in the gain of the laser) during the switching operation.

Because the cavity lifetime of the microchip laser is typically less than 1 nsec, much faster polarization switching should be obtainable if the tunable birefringent etalon could be switched more quickly. In the future we will use a faster, electro-optically tuned etalon. Polarization-switched microchip lasers may find applications in optical communications if fast polarization switching can be obtained without significant intensity spiking.

Packaging the Microchip Laser

Before a laser, or any device, can be considered useful, it must be practical: it must have the required operating characteristics, it must be an acceptable size, it must be sufficiently rugged to operate in the environment for which it is intended, and it must be affordable. The microchip laser is such a laser.

Microchip lasers are small devices (typical dimensions are less than 1 mm cubed) that can be pumped by GaAlAs diode lasers, which are even smaller. Microchip-laser packages, complete with a diode pump and piezoelectric tuner, have been assembled in an

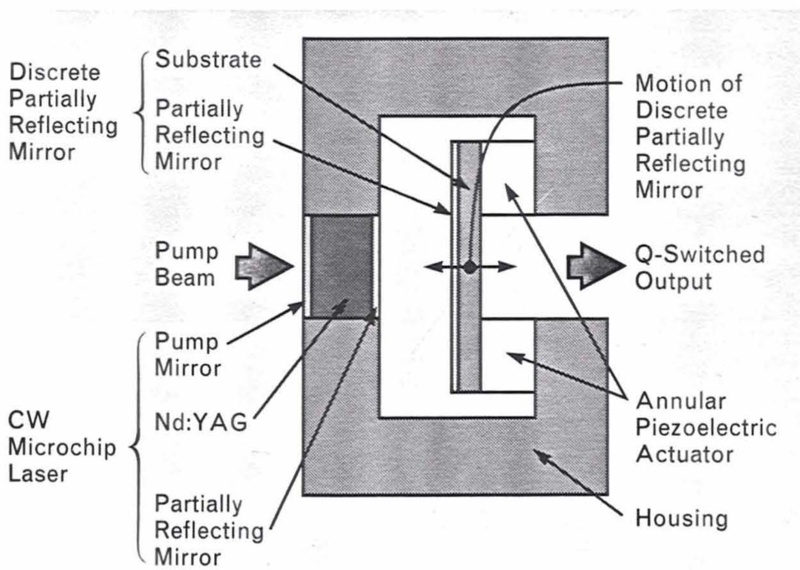

FIGURE 11. Cross section of a piezoelectrically Q-switched microchip laser. In the experiments discussed, the Nd:YAG crystal was 0.65 × 1.0 × 1.0 mm. The total distance between the pump mirror and the further of the two partially reflecting mirrors was ~1.8 mm. The piezoelectric actuator was 2.5 mm thick and had an outer diameter of 20 mm.

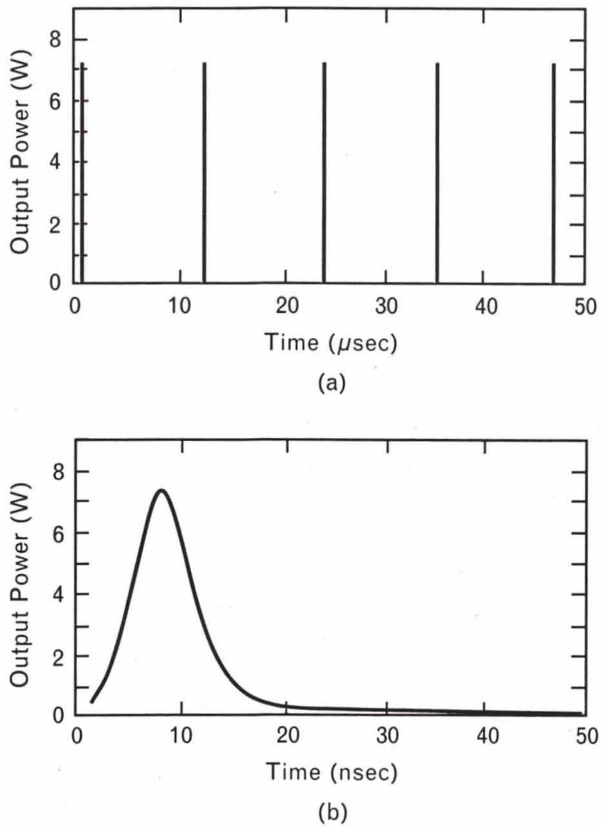

FIGURE 12. Output obtained from a 1.064-μm Q-switched Nd:YAG microchip laser: (a) train of pulses and (b) expanded time scale showing one pulse.

industry-standard TO-9 can, which occupies a volume of less than 0.35 cm^3. For more demanding

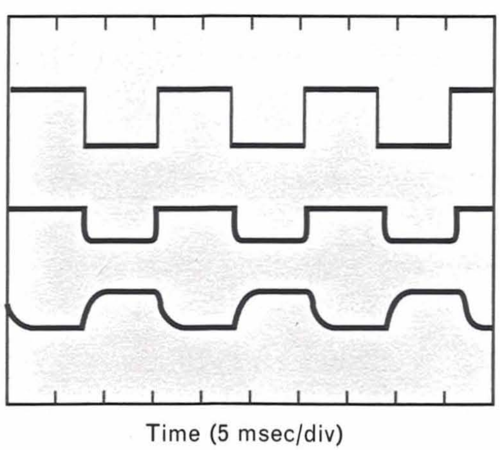

FIGURE 13. Voltage waveform (top trace) applied to the actuator of a piezoelectrically polarization-switched microchip laser and the intensity of the output in two orthogonal polarizations (middle and bottom traces). The switching times observed in the middle and bottom traces are limited by the detectors.

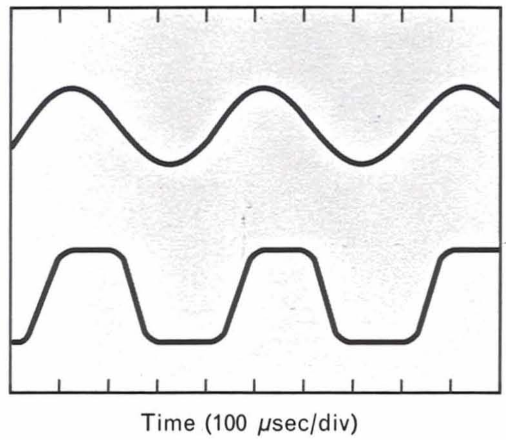

FIGURE 14. High-frequency (2.5 kHz) voltage waveform (top trace) applied to the actuator of a piezoelectrically polarization-switched microchip laser and the intensity of the output in one polarization (bottom trace). The polarization switching time of <50 μsec is shorter than the switching time of the driving waveform. No intensity spiking is seen as the polarization is switched.

applications, packages that contain the microchip laser, a pump diode, a piezoelectric tuner, a thermoelectric cooler, a temperature sensor, and a photodetector have been assembled in a TO-3 can, which occupies less than 5 cm^3 and is shown in Figure 15. The above packages are among the smallest laser packages ever assembled; they are no larger than diode laser packages.

Microchip lasers are monolithic devices in that the cavity mirrors are dielectrically coated directly onto the gain medium. There are no optics that can become misaligned. Nd:YAG is an extremely rugged material and is about two orders of magnitude less sensitive to temperature than GaAlAs. Consequently, the ambient environment in which a Nd:YAG microchip laser will operate is determined by the other components in the package, not by the microchip laser itself. Nevertheless, the entire microchip package is small enough so that it is not difficult to control the thermal environment of the package or to isolate the package from mechanical shock.

Future Directions

The study of microchip lasers and their applications has just begun. Much interesting and important research still needs to be conducted. Areas that are currently under exploration include electro-optic tuning and

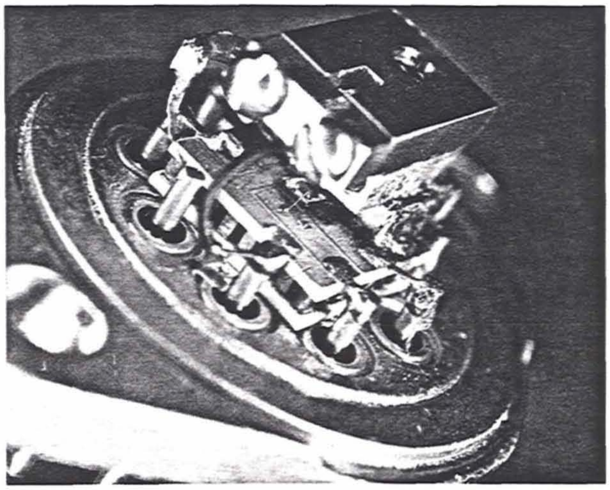

(a)

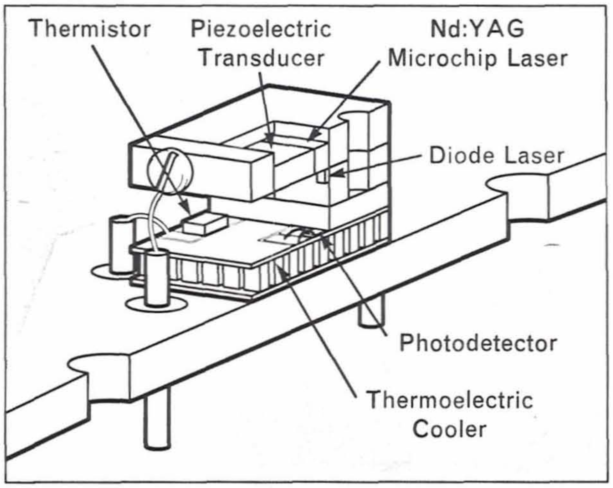

(b)

FIGURE 15. Piezoelectrically tunable microchip laser: (a) photograph and (b) illustration. The laser is mounted in a TO-3 can, which occupies less than 5 cm^3.

Q-switching, nonlinear frequency conversion, and high-power operation. These areas look promising and should open new applications for microchip lasers. Other areas of interest include the use of new gain media, different wavelengths of operation, and frequency locking for an ultrastable frequency reference.

Acknowledgments

The author thanks A. Mooradian, A. Sanchez, P.L. Kelley, and P.A. Schulz for their useful discussions. The author is also grateful to R.C. Hancock, C. Dill III, J.L. Daneu, J. Ochoa, C.D. Hoyt, and J.A. Keszenheimer for their technical contributions.

This work was sponsored by the Department of the Air Force, the Department of the Army, and the Defense Advanced Research Projects Agency.

REFERENCES

1. J.J. Zayhowski and A. Mooradian, "Single-Frequency Microchip Nd Lasers," *Opt. Lett.* 14, 24 (1989).
2. J.J. Zayhowski and A. Mooradian, "Microchip Lasers," in *OSA Proceedings on Tunable Solid State Lasers, Vol. 5*, eds. M.L. Shand and H.P. Jenssen (Optical Society of America, Washington, DC, 1989), pp. 288–294.
3. J.J. Zayhowski and A. Mooradian, "Frequency-Modulated Nd:YAG Microchip Lasers," *Opt. Lett.* 14, 618 (1989).
4. A. Owyoung and P. Esherick, "Stress-Induced Tuning of a Diode-Laser-Excited Monolithic Nd:YAG Laser," *Opt. Lett.* 12, 999 (1987).
5. P.A. Schulz, "Electro-Optic Selection and Control of Laser Frequency," in this issue.
6. J.J. Zayhowski, J. Ochoa, and A. Mooradian, "Gain-Switched Pulsed Operation of Microchip Lasers," *Opt. Lett.* 14, 1318 (1989).
7. J.J. Zayhowski and J. Keszenheimer, "Gain-Switched Diode-Pumped Microchip Lasers," *Solid State Research Report*, Lincoln Laboratory (1990:3), to be published.

JOHN J. ZAYHOWSKI
is a staff member of the Quantum Electronics Group, where he specializes in the development and applications of microchip lasers. Before joining Lincoln Laboratory five years ago, he worked at the Texas Instruments Central Research Laboratory. John received the following degrees from MIT: a joint M.S./B.S. in electrical engineering and computer science, and a Ph.D. in electrical engineering. John is a Hertz Fellow and a member of Tau Beta Pi, Eta Kappa Nu, Sigma Xi, the Optical Society of America, and the New York Academy of the Sciences.